

# Temporal Mixing

Oliver J. Smith IV, David R. Graham, and John E. Palamara  
Air Products and Chemicals, Inc., Allentown, PA 18195

DOI 10.1002/aic.10794

Published online February 14, 2006 in Wiley InterScience (www.interscience.wiley.com).

*A new method is presented for attenuating time dependent composition or temperature variations in fluid streams. We refer to this new method as temporal mixing, or mixing in time. Temporal mixing involves passing fluid streams through a vessel or configuration of vessels that exhibits a certain residence time distribution (RTD). While conventional configurations, such as a buffer tank or stirred tank, provide some attenuation, new temporal mixing configurations are described that exhibit a higher degree of attenuation. A number of simple flow configurations exhibiting limited temporal mixing are analyzed, and a theoretical configuration exhibiting ideal temporal mixing is proposed. The ideal temporal mixing configuration is characterized by a perfectly flat RTD, which totally eliminates all periodic variations at the outlet of the configuration. Although this ideal case cannot be realized in practice, a vessel that closely approximates a flat RTD is described. Simulations based on real plant data are used to show that this vessel significantly improves the attenuation achieved over that attained with conventional methods. A number of temporal mixing vessels have been installed that demonstrate improved operation and a significant reduction in operating costs for world-class hydrogen facilities. © 2006 American Institute of Chemical Engineers AIChE J, 52: 1780–1789, 2006*  
**Keywords:** temporal mixing, dampening, residence time distribution, pressure swing adsorption, frequency response

## Introduction

Material streams in which composition or temperature vary in time are common in today's chemical processing and production operations. In many cases, this variation can adversely affect the efficiency of other parts of the process. For example, in the production of hydrogen by steam methane reforming, the hydrogen is typically purified by pressure swing adsorption (PSA). PSA operates in a cyclic manner to separate a crude hydrogen feed stream into a pure hydrogen stream and a waste stream that is enriched with impurities. The concentration of the impurities in the waste stream varies periodically as the PSA progresses through its cycle. This stream is typically used as fuel to supplement the firing of the steam methane reformer. The varying of the fuel stream composition, or more precisely, its heating value, degrades the efficiency of the reformer and

causes the entire plant to operate suboptimally. Other examples of situations where variations can adversely affect system efficiency can be readily found in other cyclic or discontinuous processes, such as the smelting of ore in the primary metals industry, operation of batch chemical reactors or the venting of process upsets to buffer tanks in the chemical process industries, and variations in wastewater composition in wastewater treatment processes.

The amplitude of temperature or composition variations in a material stream can be reduced or attenuated by two well-known approaches. In one approach, heat or material is exchanged with the stream in a controlled manner to compensate for the variations. For example, heat can be added or removed to maintain a temperature set point, and in the same manner an acid or base can be added to control pH variations. This approach is often chosen when the property of interest is largely random in nature.

In another approach, the time-variant stream is introduced into a holding volume such that the natural capacitance of the volume reduces or attenuates the variation of the outlet stream

Correspondence concerning this article should be addressed to O. J. Smith at smithoj@airproducts.com.

properties relative to the inlet stream properties. In this approach, no material or energy is purposefully added to or removed from the stream. As an example of this approach for the above problem, the waste gas from a hydrogen PSA generally flows through a surge tank before it is fed to the reformer. As another example, a buffer tank can be used upstream of a reactor or other unit operation to reduce potential inlet variations. This approach is often used when the desired property varies around an average, either randomly or periodically. For this method, the variation of the outlet stream is a function of both the size and the level of mixing in the holding volume.<sup>1</sup> A high level of mixing serves to minimize spatial gradients in the holding volume and thus promotes attenuation of the amplitude variations.

We shall refer to the type of mixing that minimizes spatial gradients in the holding volume as spatial mixing. All past attempts to attenuate periodic variations using a holding volume have employed spatial mixing. In the present article, we describe a new method to attenuate variations in fluid properties. This method employs a holding volume that exhibits a type of mixing that we refer to as temporal mixing, or mixing in time. We show that an enclosed volume that exhibits ideal temporal mixing can completely eliminate periodic variations at its outlet.

In the following, we first describe temporal mixing of sinusoidal variations with ideal flow configurations. To study these ideal systems, frequency response analysis is used. Next, the analysis is extended to temporal mixing of sinusoidal variations with nonideal flow configurations. To analyze these systems, residence time distribution calculations are employed. Finally, the analysis is extended to temporal mixing of arbitrary variations with nonideal flow configurations. Here, an example is given with actual plant variations attenuated by a vessel constructed upon the principles set forth in this work. The resulting attenuation significantly improved upon the attenuation achieved previously with conventional methods.

## Ideal Transfer Functions

Methods to promote either spatial or temporal mixing in enclosed volumes can be studied by analyzing their transfer functions using frequency response analysis. For a given transfer function,  $G(s)$ , the ratio of the outlet variation amplitude to the input variation amplitude is called the amplitude ratio,  $AR$ . The  $AR$  for a sinusoidal input with frequency  $\omega$  is given by the modulus of  $G(j\omega)$ :

$$AR = |G(j\omega)| \quad (1)$$

Both the modulus and phase angle (or argument) of  $G(j\omega)$  are commonly used in the process control field for the design and analysis of feedback control systems. For the interested reader, more details on frequency response analysis is available in many process control texts (for example, see Stephanopoulos<sup>2</sup>).

The optimal configuration of continuous spatial mixing is ideal mixed flow (IMF), where the entire vessel volume is perfectly mixed and the fluid everywhere exhibits the same properties. This is the same flow pattern exhibited by an ideal continuous stirred tank reactor, when discussed in the context

of reactor engineering. The transfer function for an enclosed volume exhibiting IMF with a residence time,  $\tau = V_T/Q_T$ , is

$$G(s) = \frac{1}{\tau s + 1} \quad (2)$$

and the amplitude ratio is

$$AR = \frac{1}{\sqrt{\tau^2 \omega^2 + 1}} \quad (3)$$

Previous work has shown that sinusoidal time variations in a fluid stream can be attenuated by subjecting the stream to several ideal mixed stages in series.<sup>3</sup> The transfer function for  $N$  volumes exhibiting IMF in series is

$$G(s) = \prod_{i=1}^N \frac{1}{\tau_i s + 1} \quad (4)$$

and the amplitude ratio is

$$AR = \prod_{i=1}^N \frac{1}{\sqrt{\tau_i^2 \omega^2 + 1}} \quad (5)$$

If all the  $N$  IMF volumes are of equal size, then for an overall residence time of  $\tau$ , then

$$\tau_i = \frac{\tau}{N} \quad (6)$$

where  $\tau_i = V_i/Q_i$  is the residence time of each volume calculated based on its individual volume and volumetric flow rate (for the series configuration given here,  $Q_i = Q_T$ ). For a sinusoidal input signal with a cycle time,  $\tau_{cyc}$ ,  $\omega$  is given by

$$\omega = \frac{2\pi}{\tau_{cyc}} \quad (7)$$

The classic way to display the frequency response characteristics of a system is with Bode diagrams, which plot the logarithm of the amplitude ratio versus the logarithm of the frequency,  $\omega\tau$ . Though these diagrams could be used for describing Eqs. 3 and 5, in the results that follow the amplitude ratio can be zero. Consequently, the frequency response behavior is more appropriately displayed by a plot of amplitude ratio versus dimensionless frequency,  $\tau/\tau_{cyc}$ . As used below, this definition of dimensionless frequency allows direct comparison of the attenuation of input variations with different frequencies in processes with the same overall residence times and vice versa.

The effect of IMF volumes operated in series on the abatement of a sinusoidal input variation is shown in Figure 1. Here, the frequency responses for a single IMF volume and up to four IMF volumes in series are plotted, where each system has the same total volume. The graphic illustrates that, at small values

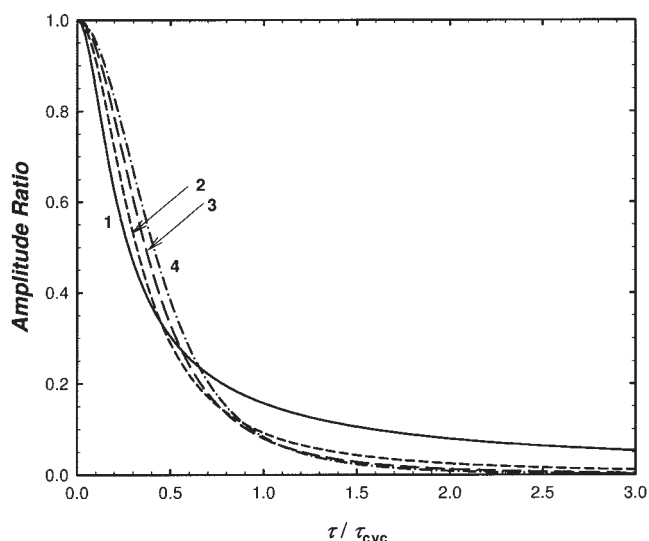


**Figure 1. Frequency response of 1, 2, 3, and 4 IMF volumes in series, where the total volume of each system is the same.**

of dimensionless frequency, a single IMF volume gives better attenuation than multiple IMF volumes in series. However, as each new volume is added, better attenuation is achieved at progressively higher dimensionless frequencies. More importantly, for any number of individual IMF volumes, an infinite total volume is needed to completely eliminate variations at the outlet ( $AR = 0$ ). Thus, although IMF volumes provide some level of attenuation, in practice a constant output stream can only be approached. Through a different flow configuration, we will show that sinusoidal flow variations can be mitigated more effectively.

One can imagine a second basic flow configuration, at the other extreme of mixing regimes, characterized by no spatial mixing. Figure 2 is a schematic of such a system that we call an Axial Plug Flow volume (APF) with a bypass. In this configuration, a material stream is split in two parts, where one part passes through a vessel and the other through a bypass. At the outlet of the vessel, the streams are recombined. In the APF portion, all elements of an inlet fluid spend the same time flowing through the enclosed volume, and thus the volume acts simply as a time delay. This is the same flow pattern exhibited by an ideal tubular-flow or plug-flow reactor, when discussed in the context of reactor engineering. In the ideal case, the bypass stream is considered to have a residence time of zero

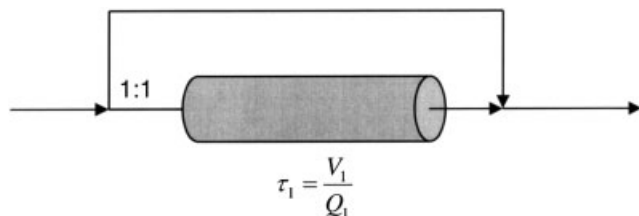


**Figure 2. Flow configuration of a single axial plug flow (APF) volume with bypass.**

The incoming stream is divided evenly between the APF volume and bypass.

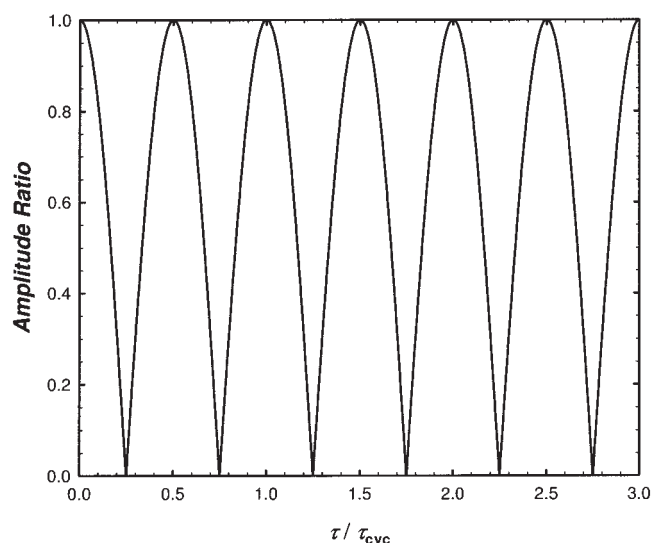


**Figure 3. Frequency response of a single APF volume with bypass.**

and is instantaneously transported to the point of remixing. For the case of equally split flow between the bypass and APF volume, the transfer function of this configuration is

$$G(s) = \frac{1}{2} [1 + \exp(-\tau_1 s)] \quad (8)$$

and the amplitude ratio is

$$AR = \frac{1}{\sqrt{2}} [1 + \cos(\omega \tau_1)]^{1/2} \quad (9)$$

where  $\tau_1 = 2\tau = 2V_T/Q_T$  is the residence time for flow through the APF volume. Here,  $\tau_1$  is larger than the overall residence time  $\tau$ , since only half of the flow passes through the APF volume. The frequency response for this configuration, given a sinusoidal input variation, is shown in Figure 3. At certain dimensionless frequencies,  $\tau/\tau_{cyc} = 0.25, 0.75, 1.25, \dots$ , the inlet variations are completely eliminated ( $AR = 0$ ), while for other dimensionless frequencies,  $\tau/\tau_{cyc} = 0.0, 0.5, 1.0, \dots$ , no attenuation is achieved ( $AR = 1$ ). The behavior of the frequency response for these particular frequencies can be understood by considering the effect of the APF volume on the inlet sinusoidal signal. The sine function exhibits its reversed mirror image symmetry about  $t = \tau_{cyc}/2$ , which is given by:

$$y(t) = -y\left(t + \frac{\tau_{cyc}}{2}\right) \quad (10)$$

When  $\tau_1 = \tau_{cyc}/2$ , the portion of the flow emerging from the APF volume is exactly  $180^\circ$  out of phase with the original signal. When the streams are remixed, the resulting phase cancellation totally eliminates the inlet variation with cycle time of  $\tau_{cyc}$ . Conversely, when  $\tau_1 = \tau_{cyc}$ , the portion of the flow emerging from the APF volume is exactly  $360^\circ$  out of phase

with the original signal. This is identical to the original signal, so that when remixed with the bypassing material the original signal is recovered. All integer multiples of the frequency ratios given above yield the prescribed response.

For APF volumes with bypass, the total elimination of all inlet variations can be achieved at a finite volume and, thus, can theoretically outperform IMF volumes. The APF performs no spatial mixing and instead relies on the concept of phase cancellation. In fact, any deviation from perfect APF behavior, such as diffusion or dispersion in the enclosed volume, will cause the two signals to have different shapes at the remixing point and, thus, perfect phase cancellation is no longer achievable. Mixing that takes advantage of phase cancellation is different from the spatial mixing described for IMF. This new type of mixing we have called temporal mixing, or mixing in time.

For example, consider an APF volume with bypass configuration where the residence time of the volume is 50 seconds ( $\tau_1 = 50$ ). Since  $\tau = \tau_1/2 = 25$ , this configuration totally eliminates sinusoidal inlet variations with cycle times, in seconds, of  $\tau_{cyc} = 100, 100/3, 100/5, 100/7, \dots$ , which correspond to the  $\tau/\tau_{cyc} = 0.25, 0.75, 1.25, \dots$  zero nodes, respectively. A single APF volume with bypass completely eliminates an infinite number of sinusoidal inlet variations of appropriate cycle time.

### Multiple APF Volumes with Bypass

The above analysis shows that certain ideal sinusoidal variations with select cycle times can be completely eliminated by a single APF volume with bypass. In contrast, most real variations observed in process streams are more complicated, and are typically comprised of arbitrary frequencies. As we progress toward how to design a configuration to eliminate variations with arbitrary frequencies, we will make use of the fact that, by performing a discrete Fourier transform, any variation, including real process plant data, can be written as a sum of sinusoidal terms. In particular, for a periodic variation with a repeat cycle time of  $\tau_{cyc}$  for which  $N_d$  equally spaced data points are available, the variations can be written by the discrete Fourier transform as the sum of  $N_d/2$  sinusoidal terms with periods of  $\tau_{cyc}, \tau_{cyc}/2, \tau_{cyc}/3, \dots, \tau_{cyc}/(N_d/2)$ . When this sequence is compared to the above result for a single APF volume with bypass, one can see that a single APF volume with bypass is able to eliminate the odd Fourier modes of a real variation, but does not affect the even modes. Here we define for a mode with period  $\tau_{cyc}/N$ , the mode is even when  $N$  is even and odd when  $N$  is odd. It will be shown that even Fourier modes are eliminated by the addition of more APF volumes, in certain configurations.

Consider the configuration given in Figure 4, in which  $N$  APF volumes are arranged in parallel with a bypass. For the case where the bypass flow is equal to the flow into each of the volumes, the transfer function of this configuration is

$$G(s) = \frac{1}{N+1} \sum_{i=0}^N \exp(-\tau_i s) \quad (11)$$

and the amplitude ratio can be found to be

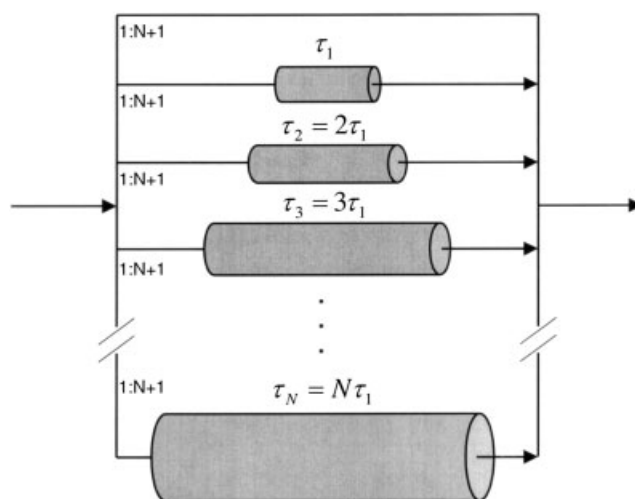


**Figure 4. Flow configuration of  $N$  APF volumes in parallel with bypass.**

The incoming stream is split evenly between the APF volumes and bypass.

$$AR = \frac{1}{N+1} \left[ \left( \sum_{i=0}^N \cos(\tau_i \omega) \right)^2 + \left( \sum_{i=0}^N \sin(\tau_i \omega) \right)^2 \right]^{1/2} \quad (12)$$

To eliminate the maximum number of Fourier modes and consequently achieve the highest level of attenuation, the  $\tau_i$ 's should be distributed such that

$$\tau_1 = \frac{\tau_2}{2} = \frac{\tau_3}{3} \dots \quad (13)$$

so that

$$\tau_i = \frac{2\tau_i}{N} \quad (14)$$

Substituting Eq. 14 into Eq. 12 yields:

$$AR = \frac{1}{N+1} \left[ \left( \sum_{i=0}^N \cos\left(\frac{2\omega\tau}{N} i\right) \right)^2 + \left( \sum_{i=0}^N \sin\left(\frac{2\omega\tau}{N} i\right) \right)^2 \right]^{1/2} \quad (15)$$

The frequency response for configurations with values of  $N$  of 2, 3, 4, and 10 is given in Figures 5a-5d. With the distribution of residence times given by Eq. 14, the APF volumes are distributed so that  $V_T = (N/2)(N+1)V_1$ . Using these equations and the values where the AR is zero and one from Figures 5a-5d, we can determine the corresponding Fourier modes that each configuration can and cannot eliminate. These are presented for the first three configurations in Table 1.

As Table 1 shows, the configuration with 2 APF volumes with bypass is able to eliminate two thirds of all the possible Fourier modes, while the configuration with 3 and 4 volumes

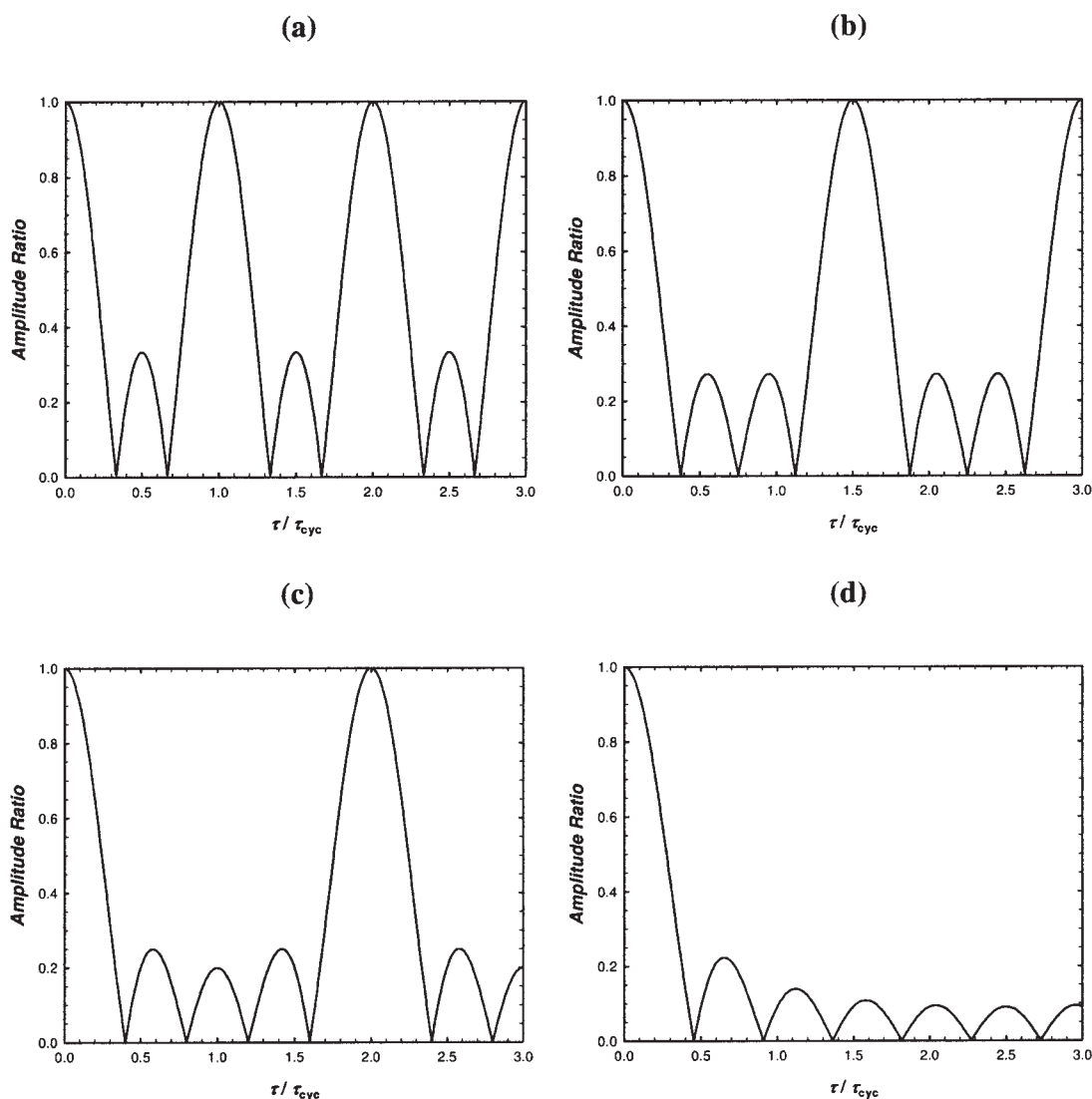


**Figure 5. Frequency response of multiple APF volumes in parallel with bypass.**

Data for  $N = 2$  (a), 3 (b), 4 (c), and 10(d) APF volumes in parallel with bypass are shown, where the total volume of each system is the same.

eliminate three fourths and four fifths, respectively. If a real inlet variation is composed of a finite number of ideal sinusoidal variations grouped around the principal mode, then a small number of APF volumes with bypass is able to totally eliminate the inlet variations. If the inlet sinusoidal variations are randomly distributed among the Fourier modes, the number of APF volumes with bypass required depends on the number of

Fourier modes. Since arbitrary variations may have an infinite number of Fourier modes, a configuration of an infinite number of APF volumes with bypass would theoretically be required to eliminate the variations.

The AR of the infinite configuration can be found by determining the limit of Eq. 15 as  $N \rightarrow \infty$ . By comparing it to a Riemann sum, this expression can be reduced to

$$AR = \frac{1}{\sqrt{2\omega\tau}} [1 - \cos(2\omega\tau)]^{1/2} \quad (16)$$

The frequency response for this configuration is given in Figure 6. It can be easily confirmed by analyzing each of the zero nodes that this configuration would eliminate all Fourier modes of an arbitrary, real inlet signal.

### Residence Time Distribution

The spatial and temporal configurations above were analyzed using frequency analysis of their transfer function. This

**Table 1. Fourier Modes Eliminated and Not Eliminated for Multiple APF Volumes with Bypass**

$N$	Modes Eliminated	Modes Not Eliminated
2	$\tau_{cyc}, \frac{\tau_{cyc}}{2}, \frac{\tau_{cyc}}{4}, \frac{\tau_{cyc}}{5}, \frac{\tau_{cyc}}{7}, \frac{\tau_{cyc}}{8}, \dots$	$\frac{\tau_{cyc}}{3}, \frac{\tau_{cyc}}{6}, \frac{\tau_{cyc}}{9}, \frac{\tau_{cyc}}{12}, \dots$
3	$\tau_{cyc}, \frac{\tau_{cyc}}{2}, \frac{\tau_{cyc}}{3}, \frac{\tau_{cyc}}{5}, \frac{\tau_{cyc}}{6}, \frac{\tau_{cyc}}{7}, \dots$	$\frac{\tau_{cyc}}{4}, \frac{\tau_{cyc}}{8}, \frac{\tau_{cyc}}{12}, \frac{\tau_{cyc}}{16}, \dots$
4	$\tau_{cyc}, \frac{\tau_{cyc}}{2}, \frac{\tau_{cyc}}{3}, \frac{\tau_{cyc}}{4}, \frac{\tau_{cyc}}{6}, \frac{\tau_{cyc}}{7}, \dots$	$\frac{\tau_{cyc}}{5}, \frac{\tau_{cyc}}{10}, \frac{\tau_{cyc}}{15}, \frac{\tau_{cyc}}{20}, \dots$

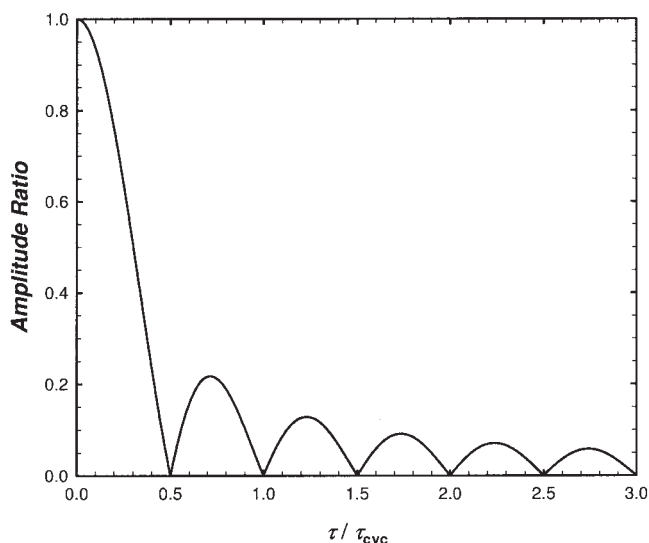


**Figure 6. Frequency response of an infinite number of APF volumes in parallel with bypass.**

type of analysis is possible for idealized APF and IMF flow patterns. However, for volumes with nonideal flow patterns, the residence time distribution (RTD) of the flow pattern can be used to determine the degree of attenuation achieved by the system

Following the terminology of Levenspiel,<sup>4</sup> the RTD of a fluid flowing through an enclosed volume can be described by a function defined as the exit age distribution or exit RTD,  $E(t)$ , where  $t$  is the time spent by an element of fluid in the volume. This exit RTD is conveniently normalized by the expression

$$\int_0^{\infty} E(t) dt = 1 \quad (17)$$

The mean residence time of the fluid in the volume,  $\tau$ , is

$$\tau = \int_0^{\infty} t E dt \quad (18)$$

Conveniently, time-variant outlet properties can be calculated from the convolution integral of the time-variant inlet properties and the RTD function by

$$C_{out}(t) = \int_0^t C_{in}(t - t') E(t') dt' \quad (19)$$

Here  $t'$  is the variable of integration, and  $C_{in}$  and  $C_{out}$  are the inlet and outlet fluid properties. The above equations assume a constant fluid flowrate through the enclosed volume. For systems with an unsteady flowrate, outlet fluid properties can be calculated in a similar manner, but the RTD may vary with absolute time.<sup>5</sup> In the present work, only constant fluid flowrate systems are considered.

When describing the residence time of an enclosed volume,

it is often convenient to use dimensionless quantities. A dimensionless time and RTD function can be defined as given by Eqs. 20 and 21, respectively.

$$\theta = \frac{t}{\tau} \quad (20)$$

$$E_{\theta} = \tau E \quad (21)$$

For these dimensionless quantities, when  $E_{\theta}$  is plotted against  $\theta$ , the area under the curve must equal 1. The dimensionless RTD functions for one, three, and an infinite number of APF volumes with bypass are given in Figures 7a-7c. The size and positions of the output pulses from the APF volumes can be determined from the residence time of each individual APF volume as compared to the mean residence time. For example, for one APF volume with bypass, the flow is equally split between the volume and the bypass. In this case, both possible paths result in pulses with areas of 1/2 and widths of 0. The bypassing material will emerge from the system at  $\theta = 0$ , followed by the material leaving the APF volume at  $\theta = 2$  (Eq. 14). A similar analysis shows that for the three APF volume configuration, four pulses with areas of 1/4 and widths of 0 result at  $\theta = 0, 2/3, 4/3, 2$ . As the number of APF volumes grows to infinity, the RTD of the system will approach that given for the infinite case shown in Figure 7c.

The RTD for the infinite case has a special shape that will be termed a flat RTD. Two distinguishing features of the flat RTD are: (1)  $E_{\theta}$  has a value of 0.5 between the dimensionless times of zero and two, and (2)  $E_{\theta}$  has a value of zero for all dimensionless times greater than two. For the flat RTD, each portion of the fluid entering the system has an equal probability of exiting at any time between  $\theta = 0$  and  $\theta = 2$ . For inlet variations of arbitrary shape and a period of  $\tau_{cyc}$ , a vessel of size  $\tau = 0.5\tau_{cyc}$  that exhibits a flat RTD will totally eliminate all variations at the outlet ( $AR = 0$ ).

A system exhibiting a flat RTD also yields good attenuation when the fluid variations are not periodic. For example, given a pulse input, the output is identical in shape to the RTD. Thus, the maximum deviation of the outlet is equal to the maximum value of the RTD. Therefore, a flat RTD exhibits the smallest maximum possible deviation. This smallest maximum deviation is two times lower than that of any number of IMF volumes in series, since their maximum deviation in the RTD is 1.

The above theoretical analysis shows that there are large benefits to be gained if a volume exhibiting a near-ideal flat RTD could be realized in a cost effective manner. However, an ideal flat RTD is only a theoretical concept, and under real conditions can only be approached. The existence of diffusion, non-uniform velocity profiles, and other natural forces would prevent a real system from achieving ideal performance. In spite of these limitations, we have developed practical designs for which the attenuation approaches that of a flat RTD. These designs are described in the next section.

## Realizing a Flat Residence Time Distribution

One possible way to develop a vessel or volume that approaches a flat residence time distribution is to build a manifold

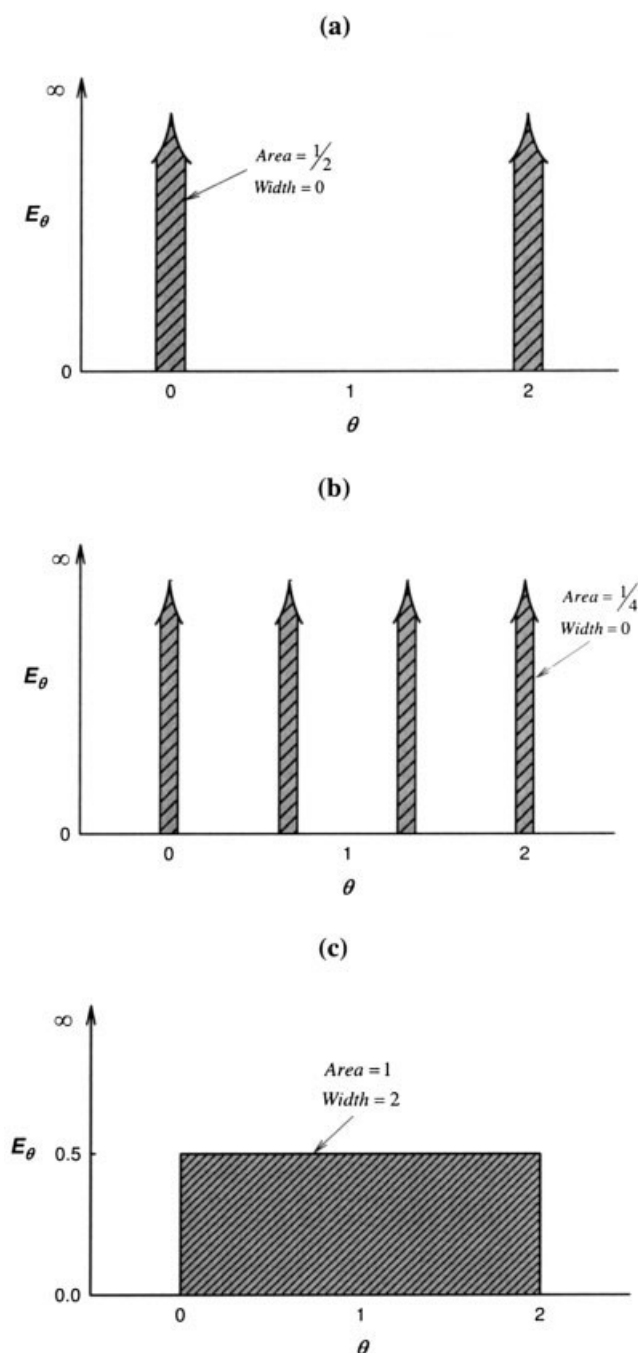


**Figure 7. Illustration of RTD of multiple APF volumes in parallel with bypass where the number of volumes is  $N = 1$  (a),  $N = 3$  (b), and  $N = \infty$  (c).**

system with parallel pipes of different volumes, as shown previously in Figure 4. The volumes of each pipe would be integer multiples of the smallest volume. As a result, if the mean residence time of the smallest pipe is  $\tau_1$ , the mean residence time of the next pipe would be  $2\tau_1$ , the next  $3\tau_1$ , and so on. Though an infinite number of pipes would be needed to achieve a perfect flat RTD, for real systems, due to diffusion and other dispersive effects, it was found that the performance of only 10 volumes exhibits the best approximation. However, for many systems, the capital cost of 10 vessels is too high.

Since cylindrical vessels normally offer the lowest capital cost per unit volume, our approach to approximating a flat RTD has been to identify potential modifications to cylindrical vessel configurations. One way to approximate a flat RTD with a cylindrical vessel is to have a tank with 10 inlets and a single outlet. If the flow volume between each inlet and the outlet exhibited axial plug flow with residence times of  $\tau_1, 2\tau_1, \dots, 10\tau_1$ , this single vessel would be equivalent to the 10 parallel vessels above. Again, the use of multiple inlets or outlets may be somewhat expensive owing to the high cost of multiple penetrations into the vessel. A more cost effective way to achieve the same results would be to use an internal inlet or outlet manifold. For example, consider the cylindrical tank with a single inlet in the bottom of the tank and an internal outlet manifold as shown in Figure 8. The fluid entering the tank would exit at different positions along the manifold. In order to approximate a flat RTD, the fluid must be equally distributed through each exit position and each must be spaced so that the mean residence time of each differs by an integer multiple (Eq. 14).

In Figure 8, the feed enters the bottom of the tank and flows upward, first through an inlet distributor, until it enters the outlet manifold through one of the holes. Flow within the outlet manifold occurs in a downward direction towards the exit at the bottom of the tank. Conceptually, it is convenient to divide the tank into imaginary sections based on different fluid velocities in the tank, as shown by the dashed lines in Figure 8. To achieve the integer multiple requirements, we require that the mean residence time of each section be the same. Since the mean residence time in each section is determined by its fluid flow and length, and the velocity is smaller at the top of the tank than at the bottom, the smallest section is at the top and the largest is at the bottom. If we assume equal distribution along the outlet manifold numbering from the top, the length of each section is given by

$$l_i = i l_1 \quad (22)$$

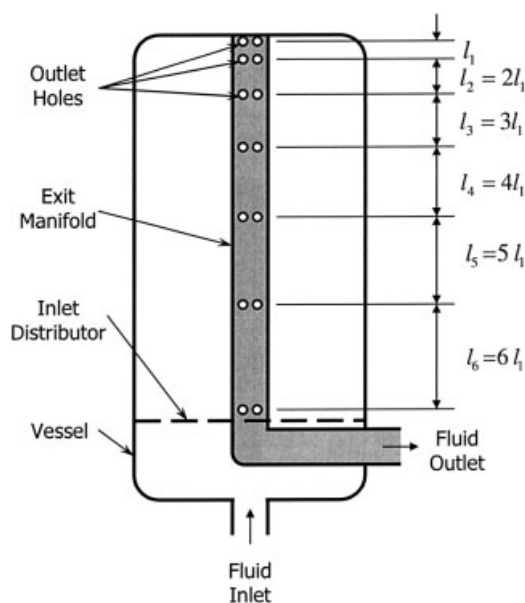


**Figure 8. Cylindrical vessel configuration used to approximate a flat RTD.**

Thus, for a vessel of length  $L$ , by summing over  $i$  we have

$$l_1 = \frac{2L}{N(N+1)} \quad (23)$$

For the configuration shown in Figure 8, there are a total of 7 unequally spaced holes in the system. If ideal APF is achieved in both the tank and the outlet manifold, this configuration is equivalent to six APF volumes in parallel with bypass.

## Residence Time Distribution of Actual Vessels

The design shown in Figure 8 represents a viable method to achieve a nearly flat RTD. To predict how this design would perform in a commercial scale vessel (3 meter diameter and 33 meter height), bench-scale laboratory experiments were performed, field data were collected, and computational fluid dynamics (CFD) models were developed.

Bench scale laboratory data were obtained by sinusoidally varying the inlet concentration to a tank, for which the configuration of the inlet and outlet manifolds could easily be changed, and measuring the subsequent outlet concentration. These experiments were performed with binary gaseous feeds, and both the tank and manifold Reynolds numbers were varied in the ranges expected for an actual plant vessel. The results from these experiments were used to validate the CFD models that are described below.

Field data were obtained by measuring both the inlet and outlet compositions for a traditional surge tank at an existing world-class hydrogen facility. These multi-component streams were analyzed with a mass spectrometer in real time to obtain compositional data. Also, the outlet stream flow rate from the surge tank was measured. The error of the flow rate measurement, though, was not as accurate as that measured for the data obtained in the laboratory.

After obtaining the above data, a computational fluid dynamics (CFD) model was developed to determine how closely vessel configurations such as that shown in Figure 8 approximate a flat RTD. Previous work has shown that RTDs for complex reactors can be efficiently predicted using CFD.<sup>6</sup> In the work performed here, a three-dimensional (3-D) CFD simulation was developed for each set of laboratory and field data. The resulting CFD simulations were found to accurately predict the observed performance for all data sets.

To match the experimental and field data, once the vessel configuration and modeling parameters were input into the CFD model, a dynamic simulation was performed by introducing the same inlet concentration profile to the model that was observed in the laboratory or field. The outlet concentrations were measured over time and compared to the experimental data. Very good predictions were found for all data sets. The RTD of the simulated vessel was also determined by introducing a tracer pulse at the inlet and recording tracer outlet concentrations over time.  $E_\theta$  was then determined by normalizing the resulting concentration versus time curve.

Next, the resulting CFD model was used to predict the performance of vessel designs similar to that shown in Figure 8. One major design parameter that needed to be determined was the optimal number of manifold sections. Figure 9 shows

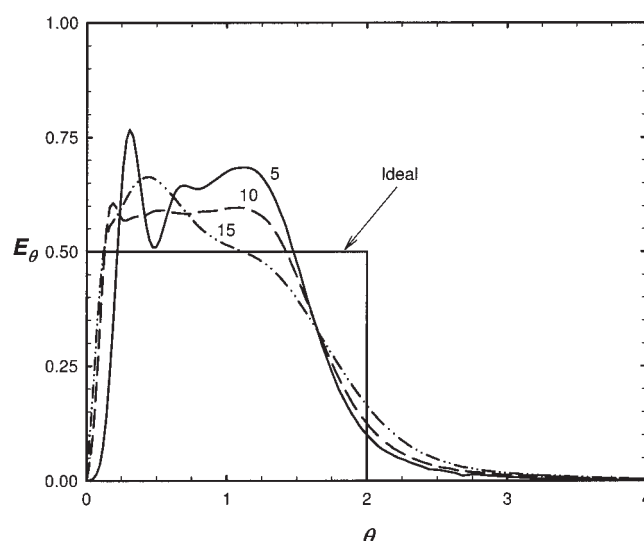


**Figure 9. RTDs resulting from CFD simulations used to analyze the vessel developed in this work.**

The RTDs for 5, 10, and 15 section vessels are shown, as well as the ideal RTD.

the predicted RTDs from CFD simulations for vessels with 5, 10, and 15 sections. As mentioned above, about 10 sections were found to optimally approximate a flat RTD.

This optimum was found as the best tradeoff between two competing effects. When a small number of sections are used, Figure 7 shows that distinct peaks in the RTD are present for APF volumes. These peaks were found to still be present even with the effects of dispersion that were included for the real volumes, as shown by the results for 5 sections in Figure 9. When a large number of sections are used, Eq. 23 shows that the length of the smallest section becomes too small to practically place an appropriately sized fluid passage in the manifold. Also, when the sections are placed too close to each other, the effects of dispersion become significant, as shown by the results for 15 sections in Figure 9.

Below, we show that the attenuation achieved for this 10 section manifold is very similar to the attenuation achieved for an ideal flat RTD. Other configurations to achieve a nearly flat RTD are described by Smith and Graham.<sup>7,8</sup>

## Attenuation Performance with Real Signals

Having identified a 10 section vessel similar in design to the drawing in Figure 8 as exhibiting a good approximation of a flat RTD, we can further extend our analysis to study its attenuation of real plant signals. To this point, frequency response analysis has been used to examine both ideal and real vessel configurations considering only a single sinusoidal inlet variation. To extend this analysis to variations of arbitrary form, it is convenient to recast such variations as a sum of sinusoidal functions. A real variation, with cycle time  $\tau_{cyc}$ , made up of only odd Fourier modes exhibits the symmetry described above by Eq. 10. Figure 3 shows that a single APF volume with bypass, with a volume of  $\tau/\tau_{cyc} = 0.25$ , is able to totally eliminate all inlet variations for this signal. On the other hand, from Figure 6 and the analysis above, we know that the odd as well as all the even Fourier modes are eliminated by

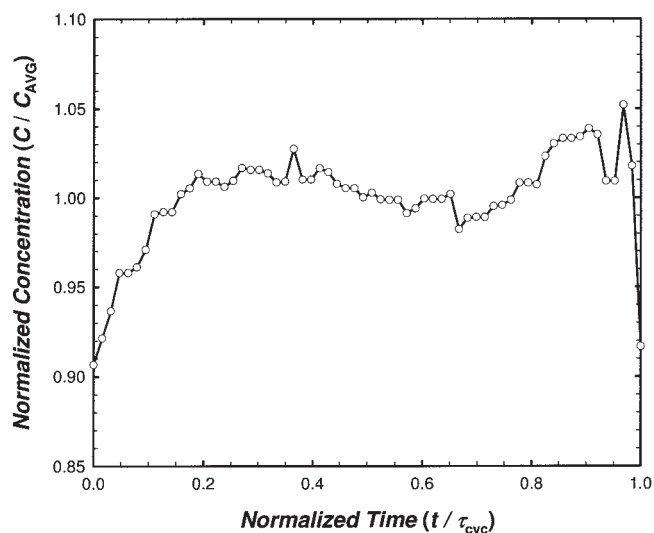


**Figure 10. Plant data concentration profile of the tail gas for a single PSA cycle.**

a flat RTD with a volume of  $\tau/\tau_{cyc} = 0.5$ . Thus, a maximum of twice the volume is needed to eliminate real signals that contain even Fourier modes. To determine whether this extra volume is worthwhile, we need to analyze the performance of these configurations for a real process signal.

The normalized concentration profile of the waste stream for one complete cycle from a hydrogen pressure swing adsorption unit is given in Figure 10. Since this profile is not perfectly symmetrical, via Eq. 10, it contains both odd and even Fourier modes. If this signal repeats perfectly in time, Figure 11 shows the AR as a function of  $\tau/\tau_{cyc}$  for a single APF volume with bypass, a vessel exhibiting a perfect flat RTD, and the 10 section vessel with the RTD shown in Figure 9. Both the vessel

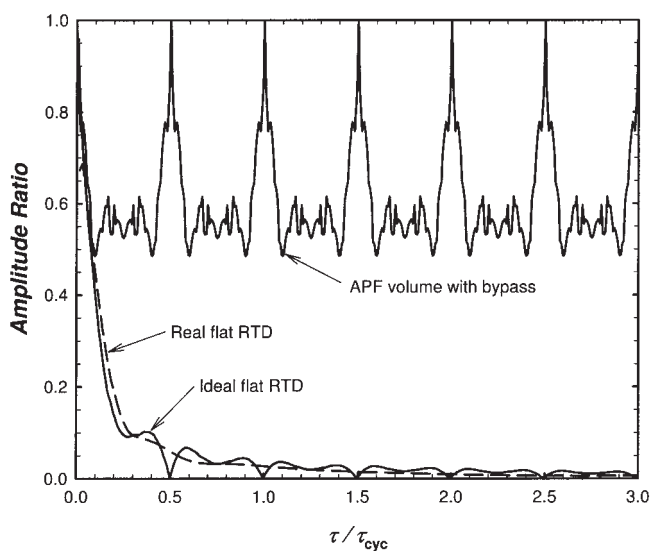


**Figure 11. Frequency response of the cylindrical vessel using the RTD determined by CFD, the ideal flat RTD, and a single APF volume with bypass, for identically repeated single cycle data shown in Figure 10.**

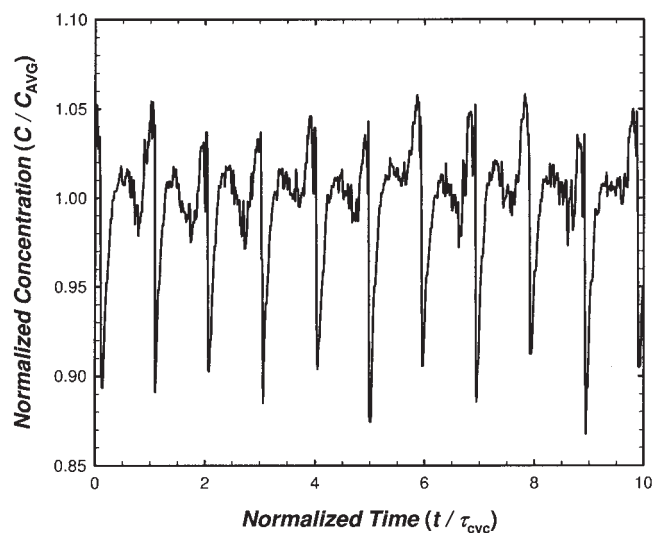


**Figure 12. Plant data concentration profile of the tail gas for 10 consecutive PSA cycles.**

with a perfect flat RTD and the 10 section vessel provide much more attenuation than the APF volume with bypass. The poor performance of the APF with bypass can be understood by comparing the results in Figure 9 with those in Figure 3 for an ideal sinusoidal input. The performance of the single APF volume with bypass in eliminating the input variations was significantly worse than for the ideal sinusoid inputs, as shown in Figure 3. This is due to the presence of even Fourier modes in the input that are not eliminated by the APF with bypass. In contrast, the performance of both the ideal flat RTD and the real flat RTD were similar to the performance expected via Figure 6. In this case, the signal was repeated perfectly in time; therefore, the ideal flat RTD completely eliminates the variations for  $\tau/\tau_{cyc} = 0.5, 1.0, 1.5, \dots$

The real plant data used in this example were created by repeating data from a single plant cycle, which thus exhibits a constant  $\tau_{cyc}$ . Real operation would not yield data with constant  $\tau_{cyc}$ . The normalized concentration profile of the waste stream for 10 continuous cycles from a hydrogen pressure swing adsorption unit is given in Figure 12. These data do not exhibit a constant  $\tau_{cyc}$  or a perfect repeat of the cycle. The attenuation performance for the same three configurations is given in Figure 13. As can be seen from the figure, a single APF volume with bypass performs poorly, while the level of variation abatement for the ideal and real flat RTD's are similar. For vessels with volumes of  $\tau = 0.5\tau_{cyc}$ , the outlet variations from a 10 section vessel approximating a flat RTD are about half that obtained from a single IMF vessel.

By comparing the performance of a single vessel that exhibits its IMF, as given in Figure 1, to the performance of a vessel of the same size that exhibits a real flat RTD, as given in Figure 13, it can be shown that at a size of  $\tau/\tau_{cyc} = 0.5$ , the real flat RTD is able to reduce the AR 300% more than the IMF vessel. This is a significant increase in performance with only a very small increase in capital. For a world-class hydrogen facility, this could save up to \$1 million/year.

Due to this superior performance of temporal mixing over other technologies, temporal mixing tanks have already been installed by Air Products and Chemicals, Inc., at eight of their

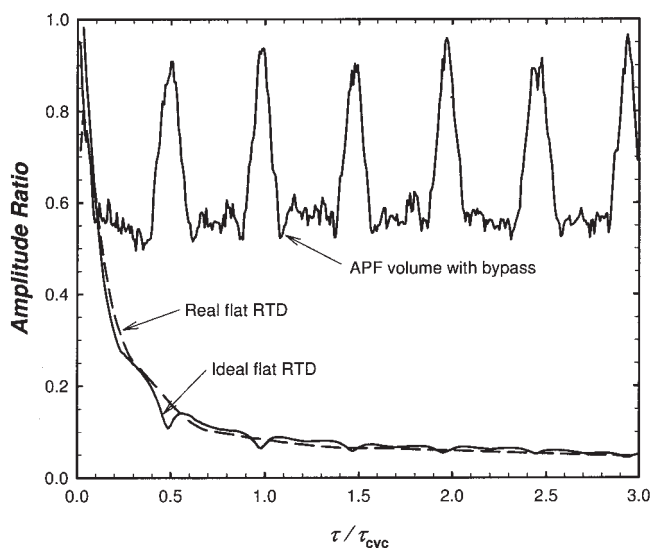


**Figure 13. Frequency response of the cylindrical vessel using the RTD determined by CFD, the ideal flat RTD, and a single APF volume with bypass, for the 10 consecutive cycle data shown in Figure 12.**

world-class hydrogen facilities. The average size of these tanks is about 450 m<sup>3</sup>, and they are the largest single pieces of equipment at the facilities. The resulting reduction in heating value swings of the waste gas to the Steam Methane Reformer allows improved operation and provides a significant reduction in operating costs.

## Conclusions

A new method to attenuate variations in fluid streams was presented that employs temporal mixing, or mixing in time. The concept of temporal mixing was developed by analyzing the performance of a number of ideal configurations. A single APF volume with bypass was shown to be able to completely eliminate a sinusoidal input consisting of only odd Fourier modes. For a sinusoidal input consisting of both even and odd Fourier modes, multiple APF volumes with bypass are required for full abatement. For a stream exhibiting an arbitrary periodic variation consisting of both even and odd Fourier modes, an ideal vessel that exhibits a flat RTD can completely eliminate the variations. Although a system exhibiting an ideal flat RTD cannot be realized, we have shown that a cylindrical vessel with a specially designed outlet manifold was able to approximate a flat RTD. CFD simulations with real plant data showed that this new design achieved nearly the same attenuation as a flat RTD, which significantly improved upon the attenuation achieved previously with conventional methods. A number of

actual vessels have been constructed, allowing improved operation and a significant reduction in operating costs for world-class hydrogen facilities.

## Acknowledgments

The authors appreciate the contributions of Xukun Luo of Air Products and Chemicals, Inc., and Nathan Shank of Lehigh University to this work.

## Notation

AR = amplitude ratio  
 $C_{in}$  = varying property of the inlet stream  
 $C_{out}$  = varying property of the outlet stream  
 $E(t)$  = exit residence time function  
 $E_g$  = dimensionless residence time distribution function  
 $G(s)$  = transfer function  
 $j = \sqrt{-1}$   
 $L$  = vessel length  
 $l_i$  = length of individual section  $i$   
 $N$  = number of volumes in a system  
 $N_d$  = number of data points in one cycle of a signal  
 $Q_i$  = volumetric flow rate through unit  $i$   
 $Q_T$  = total volumetric flow of the system  
 $t$  = time  
 $V_i$  = volume of unit  $i$   
 $V_T$  = total volume of the system

## Greek letters

$\tau$  = residence time  
 $\tau_{cyc}$  = cycle time of input signal  
 $\tau_i$  = residence time of unit  $i$   
 $\theta$  = dimensionless time  
 $\omega$  = frequency

## Abbreviations

APF = axial plug flow  
 IMF = ideal mixed flow  
 PSA = pressure swing adsorption  
 RTD = residence time distribution

## Literature Cited

1. Nagata S. *Mixing: Principles and Applications*. New York: Wiley; 1972.
2. Stephanopoulos G. *Chemical Process Control: An Introduction to Theory and Practice*. Englewood Cliffs, NJ: Prentice-Hall, Inc; 1984.
3. Hemrajani RR, Ponzi PR. U.S. Patent No. 5 156 458; 1992.
4. Levenspiel, O. *Chemical Reaction Engineering* (2nd ed). New York: Wiley; 1972.
5. Nauman EB. Residence time distribution theory for unsteady stirred tank reactors. *Chem Eng Sci*. 1969;24:1461-1470.
6. Patwardhan AW. Prediction of residence time distribution of stirred reactors. *Ind Eng Chem Res*. 2001;40:5686-5695.
7. Smith OJ, Graham DR. U.S. Patent No. 6 607 006; 2003.
8. Smith OJ, Graham DR. U.S. Patent No. 6 719 007; 2004.

Manuscript received May 11, 2005, and revision received Jan. 3, 2006.